IEEE Access
Multidisciplinary ⋮ Rapid Review ⋮ Open Access Journal

Received December 7, 2021, accepted December 20, 2021, date of publication January 6, 2022, date of current version January 14, 2022.

Digital Object Identifier 10.1109/ACCESS.2022.3140951

A Bayesian Deep Neural Network Approach to Seven-Point Thermal Sensation Perception

MUSTAFA CAKIR[1] AND AKHAN AKBULUT[2], (Member, IEEE)
[1]Department of Civil Engineering, Istanbul Kültür University, 34158 Istanbul, Turkey
[2]Department of Computer Engineering, Istanbul Kültür University, 34158 Istanbul, Turkey

Corresponding author: Mustafa Cakir (1009112001@stu.iku.edu.tr)

ABSTRACT To create and maintain comfortable indoor environments, predicting occupant thermal sensation is an important goal for architects, engineers, and facility managers. The link between thermal comfort, productivity, and health is common knowledge, and researchers have developed many state-of-the-art thermal-sensation models from dozens of research projects over the last 50 years. In addition to these, the use of intelligent data-analysis techniques, such as black-box artificial neural networks (ANNs), is receiving research attention with the aim of designing building thermal-behavior models from collected data. With the convergence of the internet of things (IoT), cloud computing, and artificial intelligence (AI), smart buildings now protect us and keep us comfortable while saving energy and cutting emissions. These types of smart buildings play a vital role in building smart cities of the future. The aim of this study is to help facility managers predict the thermal sensation of the occupants under the given circumstances. To achieve this, we applied a data-driven approach to predict the thermal sensation of occupants of an indoor environment using previously collected data. Our main contribution is to design and evaluate a deep neural network (DNN) for predicting thermal sensations with a high degree of accuracy regardless of building type, climate zone, or a building's heating and/or ventilation methods. We used the second version of the American Society of Heating, Refrigerating and Air-Conditioning Engineers (ASHRAE) Global Thermal Comfort Database to train our model. The hyperparameter-tuning process of the proposed model is optimized using the Bayesian strategy and predicts the thermal sensation of occupants with 78% accuracy, which is much higher than the traditional predicted mean vote (PMV) model and the other shallow and deep networks compared.

INDEX TERMS Thermal sensation, deep learning, deep neural network, Bayesian optimization, thermal comfort, ASHRAE Global Thermal Comfort Database II.

I. INTRODUCTION

Most people spend more than 90% of their daily lives in closed environments nowadays [1]. Considering the direct correlation between thermal comfort and productivity [2], providing proper thermal comfort for indoor environments is crucial. ASHRAE describes thermal comfort as an occupant's satisfaction with the thermal environment [3]. Fanger introduced the PMV index, which is expressed in a seven-point scale to represent the thermal sensation of an individual ranging from -3 to $+3$, corresponding to cold and hot, with 0 being neutral. According to this model, an acceptable PMV value of a thermal environment is one between -0.5 and 0.5. The other indicator of this model is the predicted percentage of dissatisfied (PPD) people; this estimates the percentage of people who would be dissatisfied in a particular environment [4]. However, it has been demonstrated that there might be differences between the PMV and actual mean vote (AMV) because of differences among individuals such as age, sex, etc. [5]. The thermal comfort of an indoor environment may have significant effects on human behavior [6]; it also defines a building's success in regard to energy consumption [7]. Studies have found that 20%–40% of the energy consumption of commercial and residential buildings results from heating, ventilation, and cooling (HVAC) operations.

There are a number of different types of HVAC control methods. One is the black-box models, which is a subcategory of model-based control methods. Black-box models are developed based on the observation of the system's input

The associate editor coordinating the review of this manuscript and approving it for publication was Yongming Li.

and output data and the development of a mathematical relationship between the input and output variables. They are developed based on observations of the system and can mathematically associate input variables to output directly [8]. Using intelligent control methods in HVAC systems produces better results compared to conventional methods [9].

By comparing intelligent methods to conventional approaches, we show that intelligent methods are better at predicting thermal sensation. We also demonstrate that deep networks outperform shallow networks.

This study is organized as follows: first, related work is introduced; then, the sample data are explained in detail. After that, how the data are processed and used for the training of the proposed model is described. Finally, we present and discuss the results of the proposed DNN model.

II. RELATED WORK

A comprehensive survey found that the use of intelligent methods has increased in recent years [10]. Afzal *et al.* aimed to maintain thermal comfort by regulating temperature and relative humidity inside an automobile. They used multiple feed-forward/feed-back propagation (MBP) artificial neural network modeling to predict the temperature and humidity inside the cabin and inform the passenger about thermal comfort [11]. Irshad *et al.* attempted to predict the thermal comfort of the occupants on a 10-point scale (-5 to $+5$) in a test room fitted with a novel thermoelectric air duct (TE-AD) cooling system instead of a standard air-conditioning system. They collected all the parameters used to calculate the PMV over a two-month period and developed an artificial neural network (ANN) model based on the Levenberg-Marquardt algorithm to predict thermal comfort. They approached this as a regression problem and achieved the best result with a single-layer 10-neuron model that produces a 0.07956 MSE (mean squared error) value [12]. Salim *et al.*, in contrast, focused on a data-shortage problem for data-driven thermal comfort models and increased the performance of thermal-comfort prediction by using the transfer learning-based multilayer perceptron model (TL-MLP). They collected data from different cities in the same climate zone to learn thermal comfort patterns and transferred this knowledge to other cities. Their study demonstrated the possibility of building thermal-comfort models with publicly available limited data [13]. A direct correlation between the minimum variable air volume (VAV) and thermal comfort was previously established [14], and for that reason, Feng *et al.* sought to create a prediction model for the valve opening of the VAV terminal based on a back propagation neural network to improve thermal comfort. They collected the actual data and trained using the newff; the results show that the error between the expected and the predicted air volume is less than 5% [15]. Ahn and Cho developed a multilayer perception-based (MLP) ANN model to optimize the supply of air conditioning to provide thermal comfort for district heating systems. They tested the proposed model on four different buildings and compared their model with the traditional on/off systems. The observed results showed that their model increased the comfort level by 27% and also reduced peak energy demands by 30% [16]. In the US, Kim and colleagues conducted an experiment to predict thermal preferences in order to provide thermal comfort. They chose to collect occupants' heating and cooling behaviors instead of utilizing a survey to train the proposed machine-learning model. They compared six different machine-learning algorithms and found that the highest level of accuracy produced was 73% by random forest (RF), which was much higher than the conventional PMV model [17]. Menassa *et al.* used a random forest (RF) classifier to predict occupants' thermal preferences in single- and multi-occupancy spaces. They trained their prediction model using a database of data collected from sensors, wearable devices, and surveys using a mobile application. The proposed model was responsible for determining the optimal condition of the space. While the RF model provided 80% classification accuracy for the thermal-preference prediction, it reduced the reports of discomfort by 53% [18]. Soh *et al.* compared the prediction accuracy of support vector machine-based (SVM) and extreme learning machine (ELM)-based classifiers to predict the three-point scale of the thermal state of occupants. They collected real-time thermal sensations of the occupants via a survey and recorded skin temperature at the same time, and they normalized skin temperature according to body-surface area and clothing insulation. They achieved a thermal-state prediction accuracy with the SVM of almost 87% [19]. Beceric-gerber *et al.* used a hidden Markov model (HMM)-based learning method to predict thermal sensation on a three-point scale by using infrared thermography of the human face as input. Their experiment with 10 subjects showed 83% accuracy for predicting uncomfortable conditions [20]. Zhang *et al.* studied the impact of the features, the amount of the data, data-processing methods and the thermal sensation scale on the prediction accuracy by using different machine-learning algorithms. They conducted their study on the same dataset that we used. The results of their study indicated that Random Forest (RF) generated the best performance among the other algorithms with 66.3% accuracy if the thermal sensation has a three-point scale and 61.1% accuracy if the thermal sensation has a seven-point scale [21].

The best classification accuracy achieved among these works is 86.7% using SVM, which demonstrates that data-driven approaches can outperform the traditional model-based approaches with a limited number of data samples. The extreme learning machine (ELM) classifier is also a good option with 79.67% prediction accuracy, according to the same study.

A comparison of the related works which are summarized above is shown in Table 1. The applied data-driven method and the outcome of that method are compared with the collected data. According to the table, shallow networks are

TABLE 1. Comparison of related works.

Study	Best algorithm	Sh/Dp	Dataset size	Metric(s)	Best score
[11] (2020)	Multiple Feed Forward Back Propagation (MBP)	Sh	19,000	Root Mean Square Error (RMSE)	0.01
[12] (2020)	Multilayer Perceptron (MLP)	Sh	1,204	Mean Square Error (MSE)	0.079
[13] (2021)	Transfer Learning-based Multilayer Perceptron model from the same Climate zone	Dp	25,000	Accuracy (%) and F1-Score (%)	54.5 and 55.12
[15] (2021)	Gradient Descent ANN	Dp	286	Mean Square Error (MSE)	0.05
[16] (2017)	Multilayer Perceptron (MLP)	Sh	8,700	Root Mean Square Error (RMSE)	0.64
[17] (2018)	Random Forest (RF)	Sh	4,743	Accuracy (%)	73
[18] (2017)	Random Forest (RF)	Sh	271	Accuracy (%)	80
[19] (2018)	Support Vector Machine (SVM)	Sh	800	Accuracy (%)	86.7
[20] (2018)	Hidden Markov Model (HMM)	Sh	457	Accuracy (%)	82.8
[21] (2020)	Random Forest (RF)	Sh	10618	Accuracy (%)	66.3

Sh: Shallow, Dp: Deep

capable of producing impressive results for thermal-comfort prediction.

III. RESEARCH METHOD

The generic solution process of data-driven prediction problems has five steps. First, the data must be collected according to this approach. There are numerous ways of collecting data; it may be preferable to sensors to collect real-time data, or data might be generated using well-known simulation tools. We collected the data from ASHRAE's second version of its Global Thermal Comfort Database published in 2018. Further details regarding the data can be found in the next subsection. As a second step, whether the problem is a regression or classification should be decided. The prediction of thermal sensation should be treated as a classification problem as it can take only the values in Figure 1, according to Fanger's model [4]. This is a way of describing the relationship between conditions of indoor environments and subjective thermal sensation. Although it creates ambiguous sensation statements like "cold" or "cool" for the evaluation of comfort, it has been used extensively since its introduction [22].

In the third step, the tool that will be used to analyze the data and develop the machine-learning model should be identified. In our study, we utilized TensorFlow, which is an end-to-end open-source platform. Then, the data must be

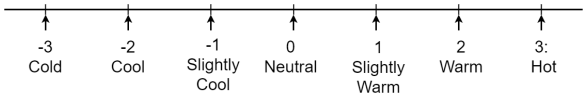

FIGURE 1. Fanger's seven-point thermal-sensation scale.

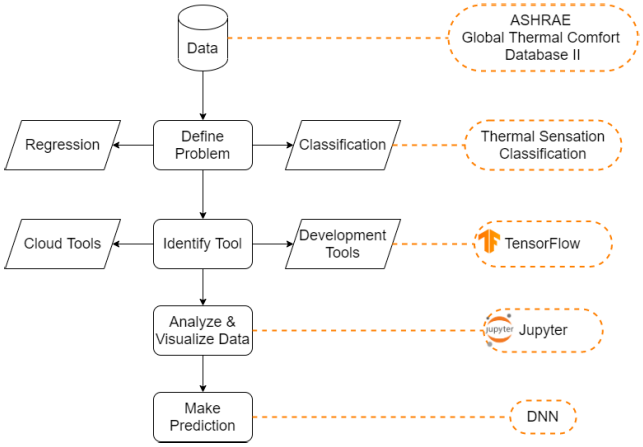

FIGURE 2. Methodology for data-driven prediction problems. Dotted shapes are the answers in our study for each question in the methodology.

visualized to obtain insights and especially to gain an idea about the distribution of numerical features. Finding the best fitting model for the given problem is an empirical process. Different algorithms with different hyperparameters should be tested as a final step until the model that creates the best predictions has been identified.

Figure 2 depicts this process as well as the activities conducted in response to each step during our research. This generic process can be applied to any kind of data-driven prediction problem.

A. DATA

As a collaborative project [23] of the University of California at Berkeley, the Dayton Foundation, the University of Sydney, Yonsei University, and the University of British Columbia, the data were collected via surveys, mobile applications, and sensors (the details are provided in Appendix B). The database covers 66 studies conducted in different countries in different seasons and with a variety of building types between 1995 and 2015. It has 107,583 data points with 51 features regardless of the different metrics of a given feature; 38 of the studies were included in our study, with 94,229 data points.

While the data for some features were collected using three sensors placed at different heights from the floor of a room for several studies, other studies were found to have collected data using one sensor for the same group of features. If a study used more than one sensor to collect data, then the average of the sensor values was considered as the actual feature value [24]. After this consolidation of sensor values, the number of the remaining features was 29. Obviously, not every study provided all the features, and this created numerous null values within the dataset. The features with high numbers of missing values were also ignored.

TABLE 2. Selected features.

Category	Feature Name	Description	Unit
Personal	Clo	Clothing ensemble insulation of the participant.	Clo
	Met	Average metabolic rate of the participant.	Met
Indoor	SET	Standard Effective Temperature	(°C)
	Air temperature	Air temperature measured of the indoor environment	(°C)
	Globe temperature	Globe temperature measured of the indoor environment	(°C)
	Air velocity	Air speed measured of the indoor environment	(m/s)
	Relative humidity	Relative humidity of the indoor environment	%
Outdoor	Outdoor monthly air temperature	Outdoor monthly average temperature when the data was collected.	(°C)

Although thermal sensation might have a limited number of observations for different classes, as mentioned in the above section, some researchers collected the data for this feature as a floating-point value with a 0.1 interval. First, we filtered and used the thermal-sensation feature with the values shown in Figure 1. Then, we added 10% tolerance, meaning that we rounded the value up or down 10% based on its nearest class. After this filtration, the remaining number of data points was 88,075 observations.

We had to remove those features with a high number of missing values, especially categorical ones such as fan, window, etc. since filling the missing values using traditional methods is difficult. We also removed several features that might be less effective for predicting thermal sensation, such as year, season, building type, etc. We ended up with the feature set shown in Table 2. Six out of eight features shown in the table are parameters for calculating the PMV value [4]. We added the SET feature as it provides more insight about the environment that the participants are in. We also added an outdoor monthly air-temperature feature to the model as an input parameter because the indoor and outdoor temperatures have either a linear or curvilinear relationship, depending on the building's heating/cooling strategy [25]. We removed all data points that have missing values and duplicate observations from the remaining features, and the dataset we wanted to use to train our model had eight features with 40,988 data points. The mean values of outdoor air temperature and clothing insulation for each climate zone can be seen in Table 3. As Table 3 shows, the study covers a range of temperatures from the lowest mean temperature, 10°C, observed in temperate oceanic and hot-summer Mediterranean climate zones to the hottest, 31.9°C, observed in a tropical wet savanna. Additionally, Table 4 displays the mean values of the indoor air temperature and relative humidity of the environment. Two major groups of factors affect occupants' thermal sensation: personal factors and environmental factors. Personal factors are the individual's metabolic rate and the insulating characteristics of his or her clothing. Environmental factors are the ambient

TABLE 3. Observed mean outdoor temperature (°C) and mean clothing insulation (clo) of all participants belongs for each climate zone.

	Outdoor Temperature		Clothing Insulation	
Climate	Mean	SD	Mean	SD
Cold semi-arid	24.5	5.4	0.6	0.2
Hot desert	22.9	6.8	0.6	0.4
Hot semi-arid	25.1	4.7	0.7	0.1
Hot-summer Mediterranean	10.9	6.4	0.8	0.3
Humid subtropical	21.6	4.7	0.6	0.3
Monsoon-influenced humid subtropical	26.1	7.1	0.8	0.3
Subtropical highland	15.3	4.7	1	0.5
Temperate oceanic	10	7.1	0.8	0.2
Tropical monsoon	26.3	1.5	0.4	0.1
Tropical wet savanna	31.9	3.6	0.7	0.1
Warm-summer Mediterranean	14.2	4.7	1	0.5

TABLE 4. Observed mean indoor air temperature (°C) and mean indoor relative humidity (%) belongs for each climate zone.

	Indoor Air Temperature		Relative Humidity	
Climate	Mean	SD	Mean	SD
Cold semi-arid	24.7	6.8	57.1	11.1
Hot desert	25.2	5.6	50.8	10.3
Hot semi-arid	27.1	3.5	47.3	13.4
Hot-summer Mediterranean	23.3	2	36.6	10.3
Humid subtropical	24.7	4.3	56.9	13.4
Monsoon-influenced humid subtropical	25.9	5.2	52.1	9.2
Subtropical highland	22.3	3.1	52.3	21.2
Temperate oceanic	24	2.3	38.8	10.6
Tropical monsoon	27.4	2.3	63.4	4.9
Tropical wet savanna	26.6	2.3	52.3	16.7
Warm-summer Mediterranean	22.3	3.1	52.3	21.2

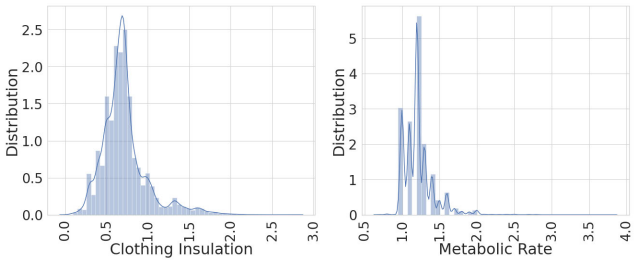

FIGURE 3. Distribution of personal factors.

temperature, relative humidity, and air velocity. In our study, we also considered the standard effective temperature (SET) and outdoor temperature as elements of the environmental factors. The data distribution of the collected personal and environmental factors is illustrated in Figures 3 and 4, which show that the majority of the parameters are close to normal (Gaussian) distribution; the remainder are definitely not. However, when we tested whether the features were in normal distribution based on D'Agostino and Pearson's hypothesis test, we had to reject the hypothesis for all features.

It has been established that, when the distribution of variables is Gaussian, many machine-learning algorithms, whether linear or nonlinear, perform better [26]. Methods

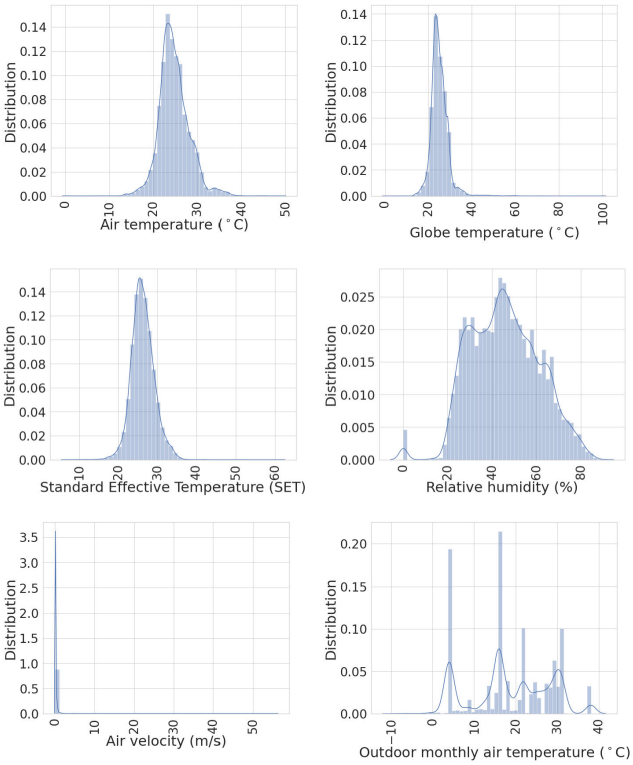

FIGURE 4. Distribution of environmental factors.

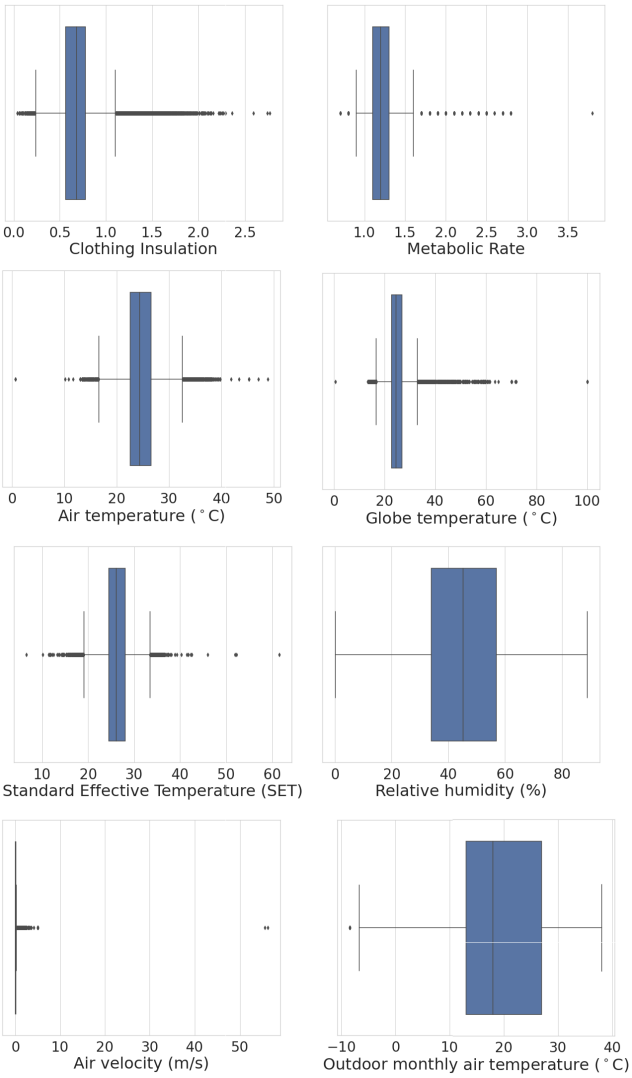

FIGURE 5. Boxplot of each feature. Dots represents the extreme values.

used to transform the variables to obtain a better Gaussian distribution are discussed in the next subsection.

B. DATA PROCESSING

We checked the dataset against the extreme values, which are called outliers. Figure 5 shows the outlier values in each feature. It's well-known that machine-learning generalization skills can be improved by detecting and removing outlier values from the dataset [26]. In order to detect the cutoff limits for each feature, we calculated the interquartile range (IQR) by subtracting the 75^{th} percentile from the 25^{th} percentile. Then we removed the IQR value from the 25^{th} percentile and added the IQR to the 75^{th} percentile to decide on the cutoff boundaries. Any values outside of the boundaries were considered outliers. This method of outlier detection can be applied to features that are not normally distributed. After removing the outliers, the remaining number of data points was 31,057. As mentioned in subsection III-A, many machine-learning algorithms perform better when the distribution of the variable is more Gaussian. It is also known that machine-learning algorithms perform better when numerical input variables are scaled to a standard range, especially algorithms that use a weighted sum of the input or that use distance measures. Different techniques can be applied depending on the collected data. We applied standard scaling (1), which can be calculated by subtracting the mean of all values of a feature from the actual value and dividing this new value to the standard deviation of that feature.

$$StandardScaling - X' = \frac{X - \mu}{\sigma} \tag{1}$$

In our study, applying the scaling technique described above to the environmental and personal factors increased the overall accuracy around 34%. Transforming the features by using MinMax scaling and Quantile transform to make the distribution more normal would increase the overall accuracy approximately 30%. For this reason, identifying the appropriate techniques to make the distribution of the data more Gaussian and, thereby, lead to the increased accuracy of the proposed model, is crucial.

As Figure 6 shows, the dataset is in a highly imbalanced state. This causes a challenge for the machine-learning algorithms due the lack of knowledge about the minority classes. Since the algorithms can't learn how to generalize these classes, both the overall accuracy and the accuracy of those classes is tainted. Synthetic Minority Oversampling Technique (SMOTE) applied to deal with this problem by generating a new example from randomly selected 2 examples in feature space of each minority class. One of them is selected randomly and the other one is a

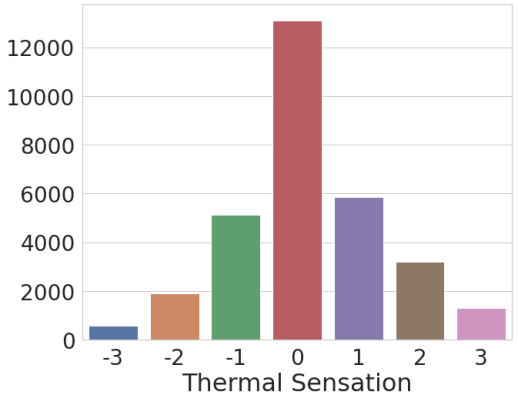

FIGURE 6. Count plot of the thermal-sensation values in the dataset.

random example from the k nearest neighbor of the first example.

C. CREATING THE DNN MODEL

A deep neural network (DNN) is an artificial neural network (ANN) with multiple layers between the input and output layers. Creating a DNN model is an empirical process; thus, we conducted different experiments to attain to the best performance. There are two parts to designing an ANN model: determining the methods of data processing and model parameters. After cleaning the data, as described in subsection III-B, we applied standard scaling to all features. However, we also conducted another experiment by applying MinMax scaling, and Quantile transform to evaluate the impact of the different data-processing methods on the model performance. We chose the Quantile transform after comparing the distribution of the features with other transformation methods such as Yeo-Johnson and box-cox power transformers. These experiments were conducted by using not only densely connected network but also one-dimensional Convolutional Neural Networks (1D CNN), which is a class of deep neural networks. Model parameters consist of two parts: model design and hyperparameters. There are different approaches determining the model parameters such as trial-and-error, grid, random, and Bayesian search. When these approaches were compared in terms of cost and space exploration skill perspective, the most beneficial was the Bayesian search, which is an optimization algorithm based on the Bayesian Theorem that finds an input that results in the minimum or maximum cost of a given objective function. This algorithm relies on conditional probability and uses two different functions. The first is a surrogate function which is the probability representation of the actual objective function and is less complicated than the actual objective function. The second one is an acquisition function which is computed from the surrogate function and used for guiding the selection of a set of hyperparameters for the next iteration. We used the Bayesian search to explore the space of the number of nodes, number of layers, cost-optimization function, learning rate, batch size, weight initializer, and dropout for DNN, along with the number of convolutional layers and filter size for each layer. We decided to use dropout for regularization to prevent the model from overfitting. The stopping criterion for the Bayesian search was 100 calls, and the best performing model parameters were found after 30 calls using DNN and 55 calls for CNN. The model that produced the best result is shown in Figure 7; it consists of one input layer that has 8 nodes as we have 8 features, 2 hidden layers with 640 nodes, and one output layer that has 7 nodes since we want to predict one class out of a seven-point thermal-sensation scale. Glorot normal, also called Xavier normal initializer method, was chosen by the search algorithm to decide on the weights at the initial step of the network. AdaMax, which is an extension of the Adaptive Movement Estimation (Adam) optimization algorithm, as the weight optimizer was determined by the search algorithm with a learning rate of 0.000001 while propagating backward on the model. We decided to use ReLU as the activation function for each layer except the last one, for which Softmax was used while propagating forward. We applied categorical cross-entropy to calculate the loss. We trained each model parameter set evaluated by the search algorithm in 500 epochs with 50 patience value as the early stopper, then validated this training using 10-fold cross-validation. In each iteration, 20% of the nodes were deleted because the dropout rate that was determined was 0.2. By contrast, for 1D CNN, the Bayesian search chose a 0.0007 learning rate, a two convolutional layers with a 103 filter size each, the Adamax weight-optimization algorithm, 'Glorot uniform for weight initializer, and 6 dense layers with 640 nodes for each. The training was completed with a 128 batch size. Further details can be seen in Figure 8. As depicted in Figure 7, the training data X consists of 8 features and N training examples. Since we used 10-fold cross-validation for the training, in each fold, 10% of the total dataset was reserved for testing the performance of the training of that particular fold. Weights W and biases b are trained using one of the gradient descent methods of the AdaMax optimizer to make predictions on thermal-sensation classes.

D. EVALUATION OF THE MODEL

As noted at the beginning of Section III, we approached the prediction of thermal sensation as a multi-class classification problem as thermal sensation defined on a seven-point scale in the sample dataset. Before creating the DNN model, we decided to evaluate the performance by checking accuracy, confusion matrix, and receiver operating characteristic (ROC) curve – area under the curve (AUC) metrics after each different model. Accuracy is derived from the confusion matrix, which is a 7×7 matrix in our case; its columns are labeled predicted classes and its rows are actual classes. Once the confusion matrix was created, each predicted class was grouped based on the four values below:

- True Positive (TP): the number of predictions where the classifier correctly predicts the actual thermal sensation;

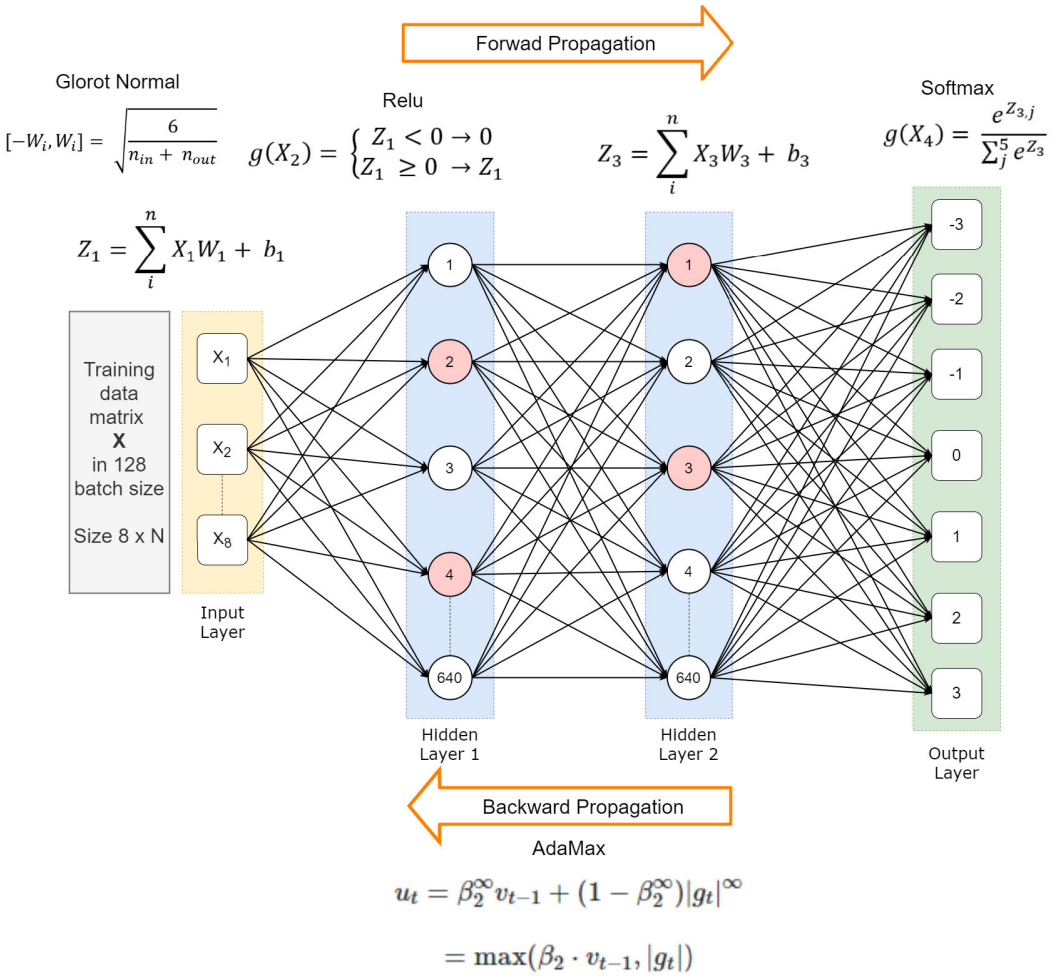

FIGURE 7. DNN architecture for predicting seven-point thermal sensation.

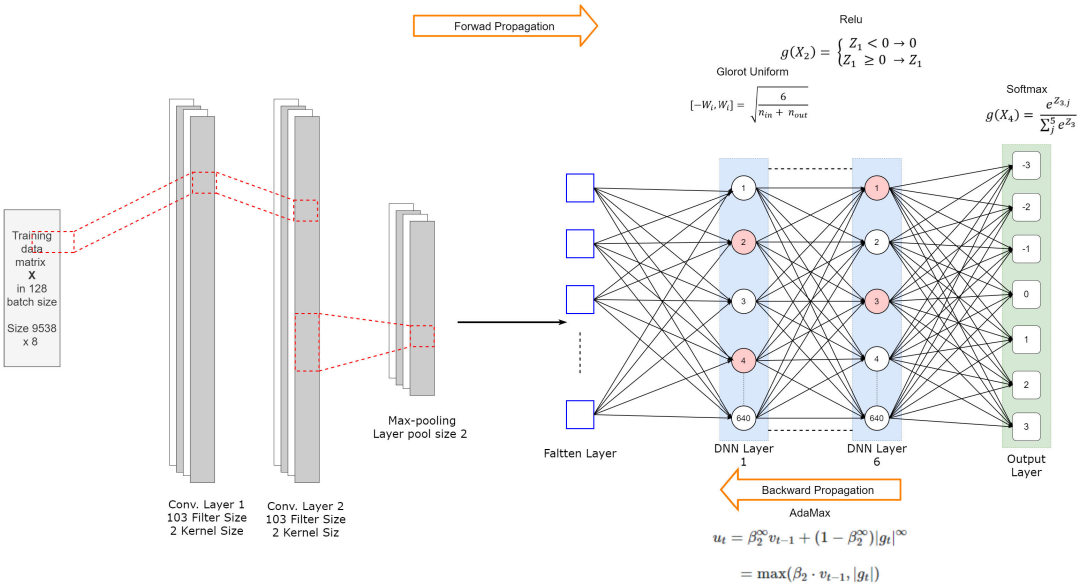

FIGURE 8. CNN architecture for predicting seven-point thermal sensation.

- False Positive (FP): the number of predictions where the classifier predicts a thermal sensation that belongs to other thermal sensation classes;
- True Negative (TN): the number of thermal sensation classes that are not predicted correctly and belong to that particular thermal sensation class; and
- False Negative (FN): the number of predicted thermal sensation classes where the classifier predicts falsely for that particular thermal sensation class.

Accuracy can be calculated for each class by dividing the total true positive and true negative values for the above-mentioned four groups (2). The overall accuracy of the model can be calculated by the number of total true positive predictions to the total number of false positive and false negative predictions (3).

$$Accuracy = \frac{TP + TN}{TP + TN + FP + FN} \tag{2}$$

$$OverallAccuracy = \frac{TotalTP}{TotalFP + TotalFN} \tag{3}$$

Two additional metrics that must be evaluated together are the ROC curve and the AUC. The ROC curve and AUC are graphical representation methods of the distinguishing ability of a classifier between all classes. The higher the AUC, the better the model is at predicting classes accurately. ROC is a probability curve that plots a true positive rate (TPR) (4) against a false positive rate (FPR) (5).

$$TPR = \frac{TP}{TP + FN} \tag{4}$$

$$FPR = \frac{FP}{FP + TN} \tag{5}$$

In addition to accuracy, confusion matrix, and ROC curve – AUC, we evaluated the precision, recall, and F1 Score metrics. Precision (6) is a metric that measures the proportion of accurately predicted classes to all other predictions for that class and is a useful metric when the classes are highly unbalanced as in our case.

$$Precision = \frac{TP}{TP + FP} \tag{6}$$

$$Recall = \frac{TP}{FN + TP} \tag{7}$$

$$F1Score = 2x\frac{PrecisionxRecall}{Precision + Recall} \tag{8}$$

Recall (7) is the ratio of the accurately predicted classes to all other classes that do not belong to that class and is also a good metric to employ when the classes are imbalanced, similar to precision. The last one is the F1 Score (8), which is the harmonic average of precision and recall. It is employed in situations where choosing between precision and recall can result in a compromise in terms of the model's false positives and false negatives.

IV. RESULTS

We performed all experiments using TensorFlow platform version 2.0, which supports GPU computing that runs on a laptop with Intel(R) Core(TM) i7-9750H 6 Core @2.60 GHz CPU, 16GB DDR4 4.5 GHz RAM memory and NVIDIA GeForce RTX 2060 6GB graphics card. The results of the proposed DNN model are promising. Our proposed model manages to predict the thermal-sensation class with 78.01% accuracy. In Figure 9, the left side represents the predicted classes, and the lower section shows the actual classes explained in the previous section.

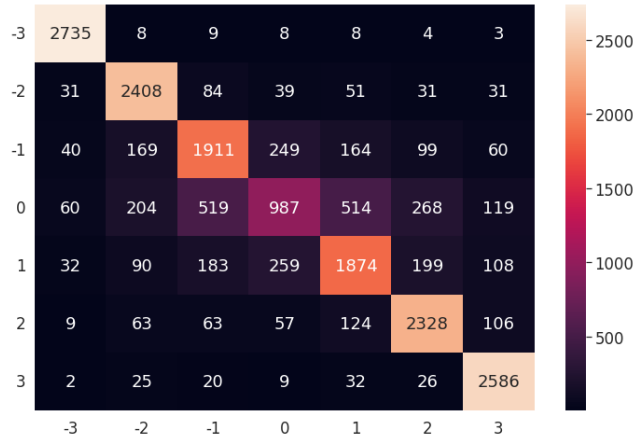

FIGURE 9. Confusion matrix of the proposed DNN model after prediction.

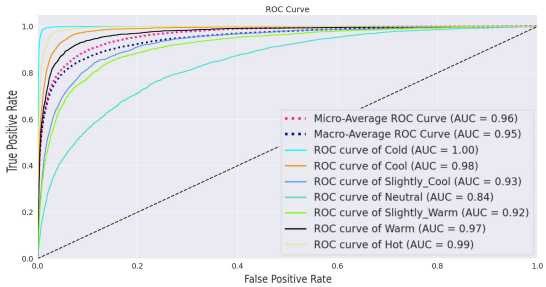

FIGURE 10. ROC curve and AUC of the proposed DNN model after prediction.

As explained in the previous section, the higher the AUC value, the better the model is at predicting classes. A circumstance where TPR equals FPR corresponds to any position on the blue line, and higher Y-axis values indicate a higher number of TPs than FNs. In our experiments, the most difficult class to distinguish from the others is "Neutral". As shown in Figure 10, it has the lowest AUC value, 0.84, while the easiest one is "Cold" with an AUC value of 1. "Hot" with an AUC of 0.99, is the second-easiest class to predict. Given that the greatest AUC value is 1, it can be asserted that the proposed model completely distinguishes the "Cold" and "Hot" classes from the rest of the classes, implying that our method can readily distinguish uncomfortable situations from the rest.

The proposed DNN model predicts the thermal sensation of the occupant with almost 78.01% accuracy, which is close to 100% better than the PMV values provided in the dataset, as it is known that PMV under predicts the thermal sensation

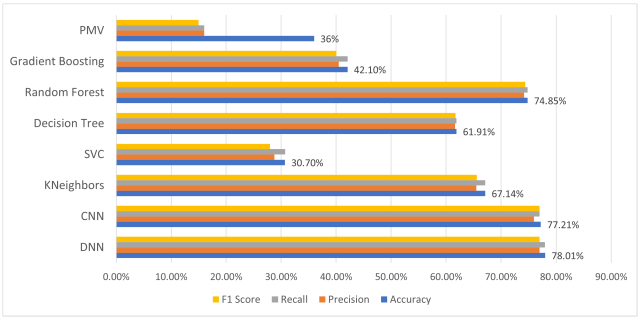

FIGURE 11. Evaluation metrics comparison of different algorithms with the same dataset.

TABLE 5. Comparison table of different methodologies.

Method	Accuracy	Precision	Recall	F1 Score
DNN	78.01%	77%	78%	77%
CNN	77.21%	76%	77%	77%
Random Forest	74.85%	74.18%	74.85%	74.42%
SVC	30.7%	28.76%	30.71%	27.97%
Decision Tree	61.91%	61.62%	61.91%	61.74%
Gradiend Boosting	42.1%	40.47%	42.1%	40.07%
KNeighbors	67.14%	61%	65.51%	65.6%
PMV	36%	16%	16%	15%

when compared to AMV [27]. This also aligns with the results of the study by Cheung *et al.* [28]. In addition, we compared the performance of the suggested model with different ANN methods. Random forest classifier is the method that provides the most similar results to our model with an accuracy score of 74.85%. This is followed by KNeighbors Classifier with a 67.14% accuracy score. The accuracy scores of the remaining methods can be seen in Figure 11. These are the prediction accuracies of each method after training with the same dataset with 10-fold cross-validation as we did during the development of our model.

As shown in Table 5, the best performance for the given dataset belongs to the DNN with an 78.01% accuracy score. Random forest classifier provides the closest accuracy score to the DNN at 74.85%. The PMV model has the lowest accuracy and precision score. Figure 11 represents the same data in bar chart format. It can also be observed that the CNN produces accuracy that is very close to the DNN method. Since the dataset that we worked on doesn't have any time stamp and is not periodical, we couldn't use ANN models such as Recurrent Neural Networks (RNN), Long Short-Term Memory (LSTM) etc., which perform better on time series.

V. DISCUSSION

The results indicate that the DNN and CNN are powerful tools for predicting the thermal sensation of occupants while using environmental factors such as indoor air temperature and relative humidity, and personal factors as inputs, even when creating a relationship between the features and the classes is difficult. Although the CNN produces slightly less accurate results than the DNN, it performs better than shallow methods and far better than the traditional PMV

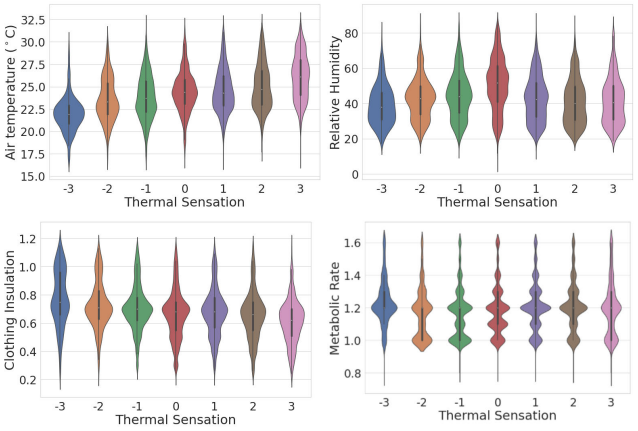

FIGURE 12. Violin plots of thermal sensation and several personal and environmental features.

model. Figure 12 defines the relationship between clothing insulation, metabolic rate, indoor air temperature, indoor relative humidity, and the thermal-sensation scale. It is clear that making inferences at a single glance is difficult due to the lack of a direct positive or negative correlation between the personal factors, environmental factors, and output. Moreover, the dataset was imbalanced as seen in Figure 6.

Figure 13 shows the relationship between (a) sex and (b) age and the thermal sensation. It can be seen that the sex of the participant has a very weak correlation to thermal-sensation perception [21]. Although age has a higher correlation than sex, it was not included in our analysis as a factor. We considered only personal factors used in the PMV calculation. We are certain that the model does not suffer from overfitting because it has a small number of layers, uses AdaMax as the weight optimizer, and has a 20% dropout rate for each layer. The experiment was undertaken with the understanding that data-driven methods outperform traditional model-based strategies, which also aligns with previous research. The results also contradict the idea that deep networks generate better results than shallow networks. The reliability of the data we trained in our ANN model is influenced by human perception. We accepted the thermal-sensation votes as valid from a statistical perspective. Figures 14 and 15 illustrate the exploration space of the Bayesian search for batch size and dropout rate. The black dots on the space represents the different combinations of model parameter sets that were trained and validated but rejected due to unsatisfactory accuracy. The Figure 15 depicts the explored batch size and learning rate combinations and the accuracy result for each combination. As figure indicates, a Bayesian search algorithm explores four different batch sizes and six different learning-rate options. Increasing the batch size has a positive impact on accuracy. Also, decreasing the learning-rate has the same impact on accuracy. As it was mentioned in subsection III-C the search repeated 100 calls; however, it reached the best accuracy score at call number 31. Any other model trained by the model parameter set derived

TABLE 6. Studies that are included to our study.

Study	Country	Climate	Purpose
[30]	Tunisia	Hot desert, Hot semi-arid, Cold semi-arid, Hot-summer Mediterranean	To develop an adaptive comfort model using linear regression which allow to estimated the indoor comfort temperature.
[31]	Brazil	Tropical monsoon	To define the relation between air velocity limits and thermal sensation.
[32]	Australia	Humid subtropical	To evaluate the feasibility of using natural ventilation along with HVAC systems.
[33]	India	Tropical wet savanna, Hot semi-arid	To develop an adaptive thermal comfort model for South India based on the collected data comparing NBC, CEN, CIBSE and ASHRAE standards.
[34]	India	Tropical wet savanna, Hot semi-arid, Monsoon-influenced humid subtropical, Subtropical highland	To develop an adaptive thermal comfort model for India by using Griffin's method and comparing it to Fanger's PMV model.
[35]	UK	Hot-summer Mediterranean	To determine the neutral indoor temperature which satisfies the 90% of the occupants and compare the results of naturally ventilated and air-conditioned environments.
[36]	France, Greece, Portugal, Sweden, UK	Temperate oceanic, Hot-summer Mediterranean, Warm-summer Mediterranean	To illustrate the actual thermal conditions in European office buildings and the occupant perceptions of those conditions by using the collected data.
[37]	China	Humid subtropical	To estimate the thermal sensation using effective temperature in buildings with split air-conditioners in hot-humid area of China as an alternative to Fanger's PMV.
[38]	China	Humid subtropical	To estimate the thermal sensation using effective temperature in naturally ventilated buildings in hot-humid area of China as an alternative to Fanger's PMV.

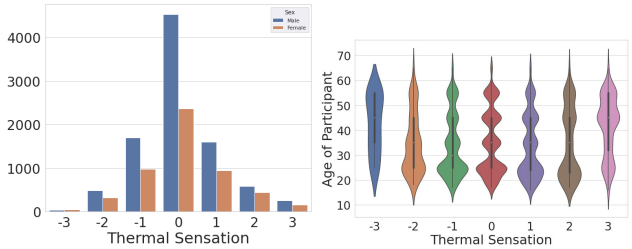

(a) Sex (b) Age

FIGURE 13. Other personal factors.

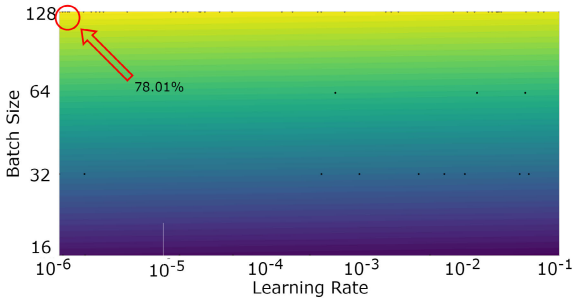

FIGURE 15. Bayesian exploration space for batch size and learning rate.

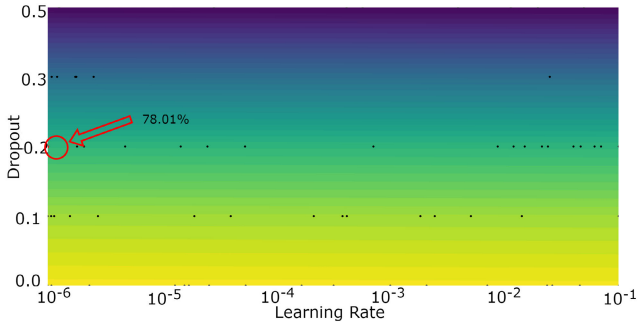

FIGURE 14. Bayesian exploration space for dropout and learning rate.

by the Bayesian search after that call, had lower accuracy. We repeated the same cycle with MinMax scaling and Quantile transformation; however, the result was 2% less than the expected.

Since the coefficients of the parameters of PMV are predetermined, the rules are set in a strict manner. For that reason, we may consider this model to be rule-based, which represents an inflexible system. However, machine-learning models are more flexible as they aim to learn the coefficients, or the rules in an inductive way. This allows researchers to create more accurate predictions for a single space or various types of spaces as the system increases generalization ability as the researchers add more data. It should be noted that the reliability of the data we trained in our deep-learning model is influenced by human perception, and therefore, the research was initiated with the assumption that the thermal-sensation votes were statistically valid. As mentioned in section IV, the most difficult class to distinguish from the others is "Neutral." One of the reasons why this class cannot be differentiated more easily is that the majority of the thermal-sensation votes provided by the subjects were affected by subjective conditions. Although personal factors such as clothing insulation and level of mobility can be measured, the effect of a person's mood on sensing the thermal environment is unknown [29].

VI. CONCLUSION

Predicting occupants' thermal sensations allows HVAC system operators to create and maintain comfortable indoor environments, which in turn have a direct correlation on productivity, and health. In this research, we introduced

TABLE 7. Features in the ASHRAE global database.

	Data	Description	Data Type	Max	Min	Mean
1	Year	Year that the data was collected.	Categorical	1995	2015	-
2	Season	Season of the year that data was collected.	Categorical	-	-	-
3	Koppen climate classification	The climate type name according to Köppen climate classification.	Categorical	-	-	-
4	Climate	The climate zone of the country from which the data is taken.	Categorical	-	-	-
5	City	City where the data was collected.	Categorical	-	-	-
6	Country	Country where the data was collected.	Categorical	-	-	-
7	Building type	Usage type of the building. Office, classroom etc.	Categorical	-	-	-
8	Cooling strategy building level	Cooling method that is used in the building.	Categorical	-	-	-
9	Cooling strategy operation mode for mixed-mode buildings	Cooling method that is used for the mixed mode buildings.	Categorical	-	-	-
10	Heating strategy building level	Heating method that is used in the building.	Categorical	-	-	-
11	Age	Age of the participant that gives the feedback.	Numeric	99	6	33
12	Sex	Gender of the participant that gives the feedback.	Categorical	-	-	-
13	Thermal sensation	Personal thermal sensation vote of the participant, from -3 (cold) to +3 (hot).	Numeric	3	-3	0.16
14	Thermal sensation acceptability	Personal vote of the participant if the thermal sensation is acceptable or not. 0 = unacceptable, 1 = acceptable.	Categorical	-	-	-
15	Thermal preference	Thermal preference of the participant. cooler, no changes, warmer.	Categorical	-	-	-
16	Air movement acceptability	Personal vote of the participant if the air movement of the indoor environment is acceptable or not. 0 = unacceptable, 1 = acceptable	Categorical	-	-	-
17	Air movement preference	Air movement preference of the participant for the indoor environment. less, no change, more	Categorical	-	-	-
18	Thermal comfort	Thermal comfort of the participant. From 1 (extremely uncomfortable) to 6 (very comfortable).	Numeric	6	0	4.3
19	PMV	Predicted Mean Vote	Numeric	3	-3	0.13
20	PPD	Predicted Percentage of Dissatisfied	Numeric	99.1	5	20.9
21	SET	Standard Effective Temperature	Numeric	61.5	6.5	25.7
22	Clo	Clothing ensemble insulation of the participant.	Numeric	2.8	0	0.6
23	Met	Average metabolic rate of the participant.	Numeric	6.8	0.6	1.2
24	activity 10	Metabolic activity of the participant in the last 10 minutes.	Numeric	3.8	0	1.1
25	activity 20	Metabolic activity of the participant between 20 and 10 minutes ago.	Numeric	6.8	0.4	1.2
26	activity 30	Metabolic activity of the participant between 30 and 20 minutes ago.	Numeric	3.8	0	1.2
27	activity 60	Metabolic activity of the participant between 30 and 60 minutes ago.	Numeric	6.8	0.6	1.3

TABLE 7. *(Continued.)* **Features in the ASHRAE global database.**

28	Air temperature (°C)	Air temperature measured of the indoor environment in Celsius degree.	Numeric	63.2	0.6	24.5
29	Ta h (°C)	Air temperature measured by the sensor which was placed at 1.1 m above the floor in Celsius degree.	Numeric	41.7	6.3	24.5
30	Ta m (°C)	Air temperature measured by the sensor which was placed at 0.6 m above the floor in Celsius degree.	Numeric	42.7	6	24.2
31	Ta l (°C)	Air temperature measured by the sensor which was placed at 0.1 m above the floor in Celsius degree.	Numeric	36.2	5	23.4
32	Operative temperature (°C)	Calculated operative temperature of the indoor environment in Celsius degree.	Numeric	44.7	6.8	24.5
33	Radiant temperature (°C)	Radiant temperature measured of the indoor environment in Celsius degree.	Numeric	148.1	1.2	24.6
34	Globe temperature (°C)	Globe temperature measured of the indoor environment in Celsius degree.	Numeric	100	0.5	24.6
35	Tg h (°C)	Globe temperature measured by the sensor which was placed at 1.1 m above the floor in Celsius degree.	Numeric	43.6	6	24.7
36	Tg m (°C)	Globe temperature measured by the sensor which was placed at 0.6 m above the floor in Celsius degree.	Numeric	46.5	3	24.3
37	Tg l (°C)	Globe temperature measured by the sensor which was placed at 0.1 m above the floor in Celsius degree.	Numeric	36.3	5.9	22.9
38	Relative humidity (%)	Relative humidity of the indoor environment.	Numeric	100	0	47.5
39	Humidity sensation	Personal vote of the participant regarding the humidity sensation of the indoor environment.3 = very dry, 2 = dry, 1 = slightly dry, 0 = just right, -1 = slightly humid, -2 = humid, -3 = very humid	Categorical	-	-	-
40	Air velocity (m/s)	Air speed of the indoor environment in meter per second.	Numeric	56.1	0	0.1
41	Velocity h	Air speed measured by the sensor which was placed at 1.1 m above the floor in meter per second.	Numeric	6.5	0	0.1
42	Velocity m	Air speed measured by the sensor which was placed at 0.6 m above the floor in meter per second.	Numeric	29.8	0	0.1
43	Velocity l	Air speed measured by the sensor which was placed at 0.1 m above the floor in meter per second.	Numeric	2.8	0	0.1
44	Subject height (cm)	Participating subject's height.	Numeric	210	99.1	167.1
45	Subject weight (kg)	Participating subject's weight.	Numeric	150	24	65.2
46	Blind (curtain)	State of blinds 0 = open, 1 = closed	Categorical	-	-	-
47	Fan	Fan mode 0 = off, 1 = on	Categorical	-	-	-
48	Window	State of windows 0 = open, 1 = closed	Categorical	-	-	-
49	Door	State of doors 0 = open, 1 = closed	Categorical	-	-	-
50	Heater	Heater mode 0 = off, 1 = on	Categorical	-	-	-
51	Outdoor monthly air temperature (°C)	Outdoor monthly average temperature when the data was collected in Celsius degree.	Numeric	45.1	-18	17.4

a DNN-based thermal-sensation prediction model that was trained and tested on data collected by ASHRAE from 66 different studies. First, we decided on the feature set to be used for the seven-point scale thermal-sensation prediction. After deleting all null values and outliers we had more than 30,000 data points to train the DNN model. We applied a Bayesian search to find hyperparameters that created the best accuracy. After training with the detected hyperparameters, the overall accuracy score that we achieved was 78%, which was higher than the other methods trained on the same dataset and the traditional PMV model. The proposed model was also shown to be suitable for the prediction of the thermal sensation, despite the facts that the input features and the output label have no direct relationship and the dataset is highly imbalanced. The proposed thermal-comfort learning method can enhance the control process of HVAC systems. In addition to our research, further studies are needed to determine the importance of other personal factors such as sex, age, weight, and height of the occupants. Taking advantage of wearable technology such as smartwatches can be considered as a future research topic in order to gain more accurate data about occupants' metabolic rates. In particular, gaining more insights into physical condition such as heart rate, blood oxygen level, or sleep patterns using smartwatches might provide an indication of the emotional state of an individual, which may in turn allow us to eliminate subjective conditions. The accuracy of the proposed model can be increased by using a dataset that has values properly labeled. Applying feature engineering methods such as dimensionality reduction or selecting a subset of the features can also have a positive impact on the model's performance. Furthermore, establishing a recommendation system for the operators of the building to help them schedule on/off times for air-conditioning systems by predicting the thermal sensation of the occupants can be utilized to achieve energy savings. Research can also be undertaken to examine the influence of real-time HVAC set-point adjustment on thermal comfort and energy savings by integrating the model with an existing HVAC system using one of the well-known communication protocols such as ZigBee or BACnet.

APPENDIX A

See Table 6.

APPENDIX B

See Table 7.

REFERENCES

[1] R. Qi, L. Lu, and H. Yang, "Investigation on air-conditioning load profile and energy consumption of desiccant cooling system for commercial buildings in Hong Kong," *Energy Buildings*, vol. 49, pp. 509–518, Jun. 2012.

[2] D. Clements-Croome and L. Baizhan, "Productivity and indoor environment," in *Proc. Healthy Buildings*, vol. 1, pp. 629–634, 2000.

[3] *Thermal Environmental Conditions for Human Occupancy*, Standard 55-2004, American Society of Heating, Refrigerating and Air-Conditioning Engineers Inc., Atlanta, Georgia, 2004.

[4] P. O. Fanger, "Thermal comfort. Analysis and applications in environmental engineering," in *International Series of Monographs on Physics, Copenhagen*. Washington, DC, USA: Danish Technical Press., 1970.

[5] L. Schellen, W. D. Van Marken Lichtenbelt, M. G. L. C. Loomans, J. Toftum, and M. H. D. Wit, "Differences between young adults and elderly in thermal comfort, productivity, and thermal physiology in response to a moderate temperature drift and a steady-state condition," *Indoor Air*, vol. 20, no. 4, pp. 273–283, Apr. 2010.

[6] G. S. Brager and R. J. de Dear, "Thermal adaptation in the built environment: A literature review," *Energy Buildings*, vol. 27, no. 1, pp. 83–96, Feb. 1998.

[7] J. F. Nicol and M. A. Humphreys, "Adaptive thermal comfort and sustainable thermal standards for buildings," *Energy Buildings*, vol. 34, no. 6, pp. 563–572, 2002.

[8] R. Kumar, R. K. Aggarwal, and J. D. Sharma, "Energy analysis of a building using artificial neural network: A review," *Energy Buildings*, vol. 65, pp. 352–358, Oct. 2013.

[9] M. Collotta, A. Messineo, G. Nicolosi, and G. Pau, "A dynamic fuzzy controller to meet thermal comfort by using neural network forecasted parameters as the input," *Energies*, vol. 7, no. 8, pp. 4727–4756, Jul. 2014.

[10] M. Çakır, A. Akbulut, and Y. Hatay Önen, "Analysis of the use of computational intelligence techniques for air-conditioning systems: A systematic mapping study," *Meas. Control*, vol. 52, nos. 7–8, pp. 1084–1094, Sep. 2019.

[11] A. Afzal, C. A. Saleel, I. A. Badruddin, T. M. Y. Khan, S. Kamangar, Z. Mallick, O. D. Samuel, and M. E. M. Soudagar, "Human thermal comfort in passenger vehicles using an organic phase change material—An experimental investigation, neural network modelling, and optimization," *Building Environ.*, vol. 180, Aug. 2020, Art. no. 107012.

[12] K. Irshad, A. I. Khan, S. A. Irfan, M. M. Alam, A. Almalawi, and M. H. Zahir, "Utilizing artificial neural network for prediction of occupants thermal comfort: A case study of a test room fitted with a thermoelectric air-conditioning system," *IEEE Access*, vol. 8, pp. 99709–99728, 2020.

[13] N. Gao, W. Shao, M. S. Rahaman, J. Zhai, K. David, and F. D. Salim, "Transfer learning for thermal comfort prediction in multiple cities," *Building Environ.*, vol. 195, May 2021, Art. no. 107725.

[14] P. Anand, C. Sekhar, D. Cheong, M. Santamouris, and S. Kondepudi, "Occupancy-based zone-level VAV system control implications on thermal comfort, ventilation, indoor air quality and building energy efficiency," *Energy Buildings*, vol. 204, Dec. 2019, Art. no. 109473.

[15] G. Feng, S. Lei, X. Gu, Y. Guo, and J. Wang, "Predictive control model for variable air volume terminal valve opening based on back-propagation neural network," *Building Environ.*, vol. 188, Jan. 2021, Art. no. 107485.

[16] J. Ahn and S. Cho, "Development of an intelligent building controller to mitigate indoor thermal dissatisfaction and peak energy demands in a district heating system," *Building Environ.*, vol. 124, pp. 57–68, Nov. 2017.

[17] J. Kim, Y. Zhou, S. Schiavon, P. Raftery, and G. Brager, "Personal comfort models: Predicting individuals' thermal preference using occupant heating and cooling behavior and machine learning," *Building Environ.*, vol. 129, pp. 96–106, Feb. 2018.

[18] D. Li, C. C. Menassa, and V. R. Kamat, "Personalized human comfort in indoor building environments under diverse conditioning modes," *Building Environ.*, vol. 126, pp. 304–317, Dec. 2017.

[19] T. Chaudhuri, D. Zhai, Y. C. Soh, H. Li, and L. Xie, "Thermal comfort prediction using normalized skin temperature in a uniform built environment," *Energy Buildings*, vol. 159, pp. 426–440, Jan. 2018.

[20] A. Ghahramani, G. Castro, S. A. Karvigh, and B. Becerik-Gerber, "Towards unsupervised learning of thermal comfort using infrared thermography," *Appl. Energy*, vol. 211, pp. 41–49, Feb. 2018.

[21] M. Luo, J. Xie, Y. Yan, Z. Ke, P. Yu, Z. Wang, and J. Zhang, "Comparing machine learning algorithms in predicting thermal sensation using ASHRAE comfort database II," *Energy Buildings*, vol. 210, Mar. 2020, Art. no. 109776.

[22] M. Schweiker, X. Fuchs, S. Becker, M. Shukuya, M. Dovjak, M. Hawighorst, and J. Kolarik, "Challenging the assumptions for thermal sensation scales," *Building Res. Inf.*, vol. 45, no. 5, pp. 572–589, Jul. 2017.

[23] V. F. Ličina *et al.*, "ASHRAE global thermal comfort database II," *Methods*, vol. 2020, pp. 6–24, 2021.

[24] C. C. Benton and G. S. Brager, *Sunset Building: Final Report: A Study of Occupant Thermal Comfort in Support of Pg&e's Advanced Customer Technology Test (Act2) for Maximum Energy Efficiency*. New York, NY, USA: Center for Environmental Design Research, 1994.
[25] F. Nicol, H. B. Rijal, H. Imagawa, and R. Thapa, "The range and shape of thermal comfort and resilience," *Energy Buildings*, vol. 224, Oct. 2020, Art. no. 110277.
[26] J. Brownlee, *Data Preparation for Machine Learning: Data Cleaning, Feature Selection, and Data Transforms in Python*. Machine Learning Mastery, 2020.
[27] A. Beizaee, S. Firth, K. Vadodaria, and D. Loveday, "Assessing the ability of PMV model in predicting thermal sensation in naturally ventilated buildings in U.K.," in *Proc. 7th Windsor Conf., Changing Context Comfort Unpredictable World*, London, U.K., Apr. 2012, p. 17.
[28] T. Cheung, S. Schiavon, T. Parkinson, P. Li, and G. Brager, "Analysis of the accuracy on PMV–PPD model using the ASHRAE global thermal comfort database II," *Building Environ.*, vol. 153, pp. 205–217, Apr. 2019.
[29] H. Wang and L. Liu, "Experimental investigation about effect of emotion state on people's thermal comfort," *Energy Buildings*, vol. 211, Mar. 2020, Art. no. 109789.
[30] C. Bouden and N. Ghrab, "An adaptive thermal comfort model for the Tunisian context: A field study results," *Energy Buildings*, vol. 37, no. 9, pp. 952–963, Sep. 2005.
[31] C. M. Candido, "Indoor air movement acceptability and thermal comfort in hot-humid climates," M.S. thesis, Center Built Environ., UC Berkeley, Berkeley, CA, USA, 2010. [Online]. Available: https://escholarship.org/uc/item/78v8055h
[32] S. Drake, R. de Dear, A. Alessi, and M. Deuble, "Occupant comfort in naturally ventilated and mixed-mode spaces within air-conditioned offices," *Architectural Sci. Rev.*, vol. 53, no. 3, pp. 297–306, Aug. 2010.
[33] M. Indraganti, R. Ooka, H. B. Rijal, and G. S. Brager, "Adaptive model of thermal comfort for offices in hot and humid climates of India," *Building Environ.*, vol. 74, pp. 39–53, Apr. 2014.
[34] S. Manu, Y. Shukla, R. Rawal, L. E. Thomas, and R. de Dear, "Field studies of thermal comfort across multiple climate zones for the subcontinent: India model for adaptive comfort (IMAC)," *Building Environ.*, vol. 98, pp. 55–70, Mar. 2016.
[35] N. A. Oseland, J. Reardon, and G. Langkilde, "Acceptable temperature ranges in naturally ventilated and air-conditioned offices/discussion," *Ashrae Trans.*, vol. 104, p. 1018, Oct. 1998.
[36] J. L. Stoops, "The thermal environment and occupant perceptions in European office buildings," M.S. thesis, Dept. Building Services Eng., Chalmers Univ. Technol., Goteborg, Sweden, 2002.
[37] Y. Zhang, H. Chen, and Q. Meng, "Thermal comfort in buildings with split air-conditioners in hot-humid area of China," *Building Environ.*, vol. 64, pp. 213–224, Jun. 2013.
[38] Y. Zhang, J. Wang, H. Chen, J. Zhang, and Q. Meng, "Thermal comfort in naturally ventilated buildings in hot-humid area of China," *Building Environ.*, vol. 45, no. 11, pp. 2562–2570, Nov. 2010.

MUSTAFA CAKIR received the B.S. and M.S. degrees in computer engineering from Istanbul Kültür University (IKU), Turkey, in 2005 and 2010, respectively, where he is currently pursuing the Ph.D. degree. He was a Research Assistant with the Department of Computer Engineering, IKU, from 2005 to 2007. After that, he worked as a senior software engineer and a solution architect for the industry leader of pay TV operators in Turkey for four years. Since 2011, he has worked as the project manager. His current research interests include the use of intelligent methods in energy efficiency and thermal comfort of HVAC systems.

AKHAN AKBULUT (Member, IEEE) received the B.S. and M.S. degrees in computer engineering from Istanbul Kültür University (IKU), Turkey, in 2001 and 2008, respectively, and the Ph.D. degree in computer engineering from Istanbul University, Turkey, in 2013. From 2004 to 2013, he was a Research Assistant with the Department of Computer Engineering, IKU, where he was an Assistant Professor from 2013 to 2017. From 2017 to 2019, he was a Postdoctoral Researcher with the Department of Computer Science, North Carolina State University, NC, USA. In 2019, he rejoined the Department of Computer Engineering, IKU, where he was promoted to an Associate Professor. He is currently the Chairman of the Department of Computer Engineering, IKU. His current research interests include design and performance optimization of software-intensive systems, machine-learning applications, Internet architectures, and broadening participation in cloud computing research.